Optimal Eigenbeamforming for Suppressing Self-Interference in Full-Duplex MIMO Relays

Taneli Riihonen†, Arun Balakrishnan†, Katsuyuki Haneda†, Shurjeel Wyne*, Stefan Werner†, and Risto Wichman†
†SMARAD Centre of Excellence, Aalto University School of Electrical Engineering, Finland
*COMSATS Institute of Information Technology, Islamabad, Pakistan
Contact email: taneli.riihonen@aalto.fi

***Abstract*—We address the main technical challenge encountered in the practical implementations of full-duplex MIMO relays, i.e., how to mitigate efficiently the self-interference that loops back from the relay's transmit antenna array to its receive antenna array. In particular, we consider spatial-domain suppression using optimal eigenbeamforming that minimizes the power of the residual self-interference signal by pointing the transmit and receive beams to the minimum eigenmodes of the self-interference channel. As a special case, the scheme covers also the null-space projection approach discussed in earlier papers. To demonstrate the feasibility of full-duplex relaying, we have previously built prototype antenna arrays for a full-duplex MIMO relay and measured an extensive set of real-world self-interference channels in different deployment scenarios. Using the measurement data, we now evaluate the natural isolation between separated antenna arrays and the additional isolation given by optimal eigenbeamforming.**

I. Introduction

The theory of full-duplex MIMO relays has been widely studied, see, e.g., [1]–[5]. However, earlier literature typically neglects a significant practical problem: Full-duplex relays are subject to undesired self-interference because the relay uses one frequency band for simultaneous reception and transmission. In particular, the relay needs to be equipped with two antenna arrays, and dedicate one for reception and the other for transmission, in order to cope with the limited dynamic range of the receiver front-end and to facilitate digital signal processing for interference mitigation. This provides natural isolation due to free-space propagation loss, antenna directivity, and potential obstacles blocking the line-of-sight.

Our studies on SISO relays [6]–[8] demonstrate that full-duplex relays can be superior to half-duplex relays even with residual self-interference. In particular, full-duplex relay links can achieve doubled symbol rate when compared to their half-duplex counterparts where self-interference is avoided by allocating different time slots for relay reception and transmission. Consequently, doubled symbol rate renders significantly improved spectral efficiency provided that residual self-interference is kept at a low level. This motivates to develop and analyze mitigation schemes also for MIMO relays.

The variety of potential mitigation schemes is wide in the case of MIMO relays. Recent literature studies schemes ranging from time-domain cancellation [9]–[13] to different variations of spatial-domain suppression such as minimum mean square error filtering [12], null-space projection [12]–[16], antenna selection [17], eigenbeam selection [18], and the usage of receive and transmit antennas with orthogonal polarizations [19]. After all other countermeasures, smart relay gain (or transmit power) control is important for minimizing the effect of residual self-interference [20], [21].

The focus of this paper is on spatial suppression techniques. In particular, we consider optimal eigenbeamforming that points the transmit and receive beams to the minimum eigenmodes of the self-interference channel. The scheme offers significant improvement w.r.t. the earlier scheme of [18] by supporting more spatial streams without increasing the residual self-interference power. As a special case, the scheme covers also the null-space projection approach of [12], [13].

The first channel measurements for full-duplex MIMO relays are reported in [22], [23]. Using the data of [23] for outdoor-to-indoor relaying at 2.6GHz band, we illustrate herein the preliminary natural isolation arising from the directivity and spatial separation of the antenna arrays and evaluate the additional isolation given by optimal eigenbeamforming.

II. System Model and Experimental Setups

We study wireless communication from a source (S) node to a destination (D) node with the aid of a *full-duplex MIMO relay* (R) node as shown in Fig. 1. In contrast to many earlier papers, *the novel aspect in our model is to take into account the relay self-interference* as it is unavoidable in full-duplex operation. Hence, we assume that the relay is equipped with two antenna arrays (one for receiving and the other for transmitting) to obtain some preliminary natural isolation before applying signal processing for interference mitigation.

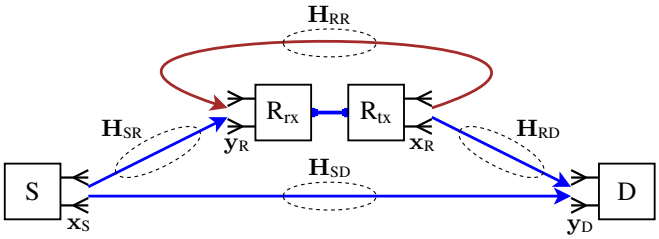

Fig. 1. Full-duplex MIMO relay link with self-interference.

†This work was partially funded by the Academy of Finland.

978-1-4244-9848-2/11$26.00©2011 IEEE

A. Signal Model

Let the source and the destination have N_{S} transmit and N_{D} receive antennas, respectively, and the relay have N_{rx} receive and N_{tx} transmit antennas. As shown in Fig. 1, matrices $\mathbf{H}_{\mathrm{SR}} \in \mathbb{C}^{N_{\mathrm{rx}} \times N_{\mathrm{S}}}$, $\mathbf{H}_{\mathrm{SD}} \in \mathbb{C}^{N_{\mathrm{D}} \times N_{\mathrm{S}}}$, $\mathbf{H}_{\mathrm{RR}} \in \mathbb{C}^{N_{\mathrm{rx}} \times N_{\mathrm{tx}}}$, and $\mathbf{H}_{\mathrm{RD}} \in \mathbb{C}^{N_{\mathrm{D}} \times N_{\mathrm{tx}}}$ represent the respective MIMO channels from the source to the relay, from the source to the destination, from the relay transmit array to the relay receive array, and from the relay to the destination. They are assumed to remain time-invariant during the transmission of each data symbol.

The relay receives and transmits simultaneously on the same frequency causing a feedback loop through the channel $\mathbf{H}_{\mathrm{RR}}$ that is not completely blocked in practice despite the antenna separation that provides natural isolation. During each channel use, the source and the relay transmit $\mathbf{x}_{\mathrm{S}} \in \mathbb{C}^{N_{\mathrm{S}} \times 1}$ and $\mathbf{x}_{\mathrm{R}} \in \mathbb{C}^{N_{\mathrm{tx}} \times 1}$, respectively, and the relay and the destination receive

$$\mathbf{y}_{\mathrm{R}} = \mathbf{H}_{\mathrm{SR}}\mathbf{x}_{\mathrm{S}} + \mathbf{H}_{\mathrm{RR}}\mathbf{x}_{\mathrm{R}} + \mathbf{n}_{\mathrm{R}} \in \mathbb{C}^{N_{\mathrm{rx}} \times 1}, \quad (1)$$

$$\mathbf{y}_{\mathrm{D}} = \mathbf{H}_{\mathrm{RD}}\mathbf{x}_{\mathrm{R}} + \mathbf{H}_{\mathrm{SD}}\mathbf{x}_{\mathrm{S}} + \mathbf{n}_{\mathrm{D}} \in \mathbb{C}^{N_{\mathrm{D}} \times 1}, \quad (2)$$

respectively. In (1), $\mathbf{H}_{\mathrm{RR}}\mathbf{x}_{\mathrm{R}}$ is the relay self-interference term to be mitigated, and $\mathbf{n}_{\mathrm{R}} \in \mathbb{C}^{N_{\mathrm{rx}} \times 1}$, $\mathbf{n}_{\mathrm{D}} \in \mathbb{C}^{N_{\mathrm{D}} \times 1}$ represent additive receiver noise components.

B. Experimental Antenna Arrays for Full-Duplex Relays

We have built receive and transmit antenna arrays for a prototype full-duplex MIMO relay and conducted a measurement campaign to obtain samples of the self-interference channel $\mathbf{H}_{\mathrm{RR}}$ in practical outdoor-to-indoor relaying scenarios. Detailed descriptions of the experimental full-duplex relay and measurement setups are provided in [23]. Herein, the measurement data is exploited for evaluating the natural isolation arising from antenna directivity and spatial separation as well as the additional isolation given by the eigenbeamforming scheme tailored for mitigating the self-interference.

Each antenna array comprises two dual-polarized square patch antennas placed over a rectangular ground plate. The arrays are identical except that transmit polarizations are slanted 45 degrees w.r.t. receive polarizations to improve natural isolation slightly. Coupling between the antenna feeds is verifiably low which allows to form four orthogonal spatial beams at both arrays. With this background in experiments, we consider the case $N_{\mathrm{rx}} = N_{\mathrm{tx}} = 4$ in all numerical results.

The channel measurement data covers two configurations:

- In the *compact array configuration*, the arrays are attached side by side (while facing opposite directions) using plastic spacers. By placing the transceiver electronics between the arrays, the complete relay device becomes a small box that is about the same size as typical Wi-Fi routers. The samples of the channel $\mathbf{H}_{\mathrm{RR}}$ are measured by deploying the relay at several locations in a meeting room such that the receive array points outdoors through windows and the transmit array provides indoor coverage.
- In the *separate array configuration*, the receive array is deployed on the outer side of a meeting room window such that it points outwards. The samples of the channel $\mathbf{H}_{\mathrm{RR}}$ are measured by deploying the transmit array at various locations in the same room (line-of-sight, LOS, channel) and in the adjacent corridor (non-line-of-sight, NLOS, channel). The measurements include four array orientations, see Fig. 2: Orientations 1 and 2 represent the case where the transmit array is perpendicular to the receive array; Orientation 3 points the main beam of the transmit array towards the receive array; and Orientation 4 points the two arrays in opposite directions.

For reference, we also show numerical results for *simulated MIMO Rayleigh channels* with independent and identically distributed circularly-symmetric complex Gaussian elements.

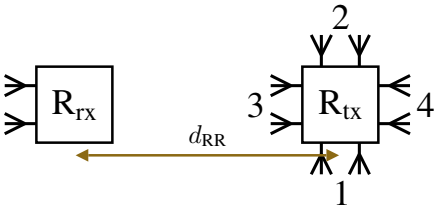

Fig. 2. Four orientations for the relay transmit antenna array ($\mathrm{R_{tx}}$) w.r.t. the relay receive antenna array ($\mathrm{R_{rx}}$) in the experiments with the separate array configuration (d_{RR} denotes the distance between the arrays). The compact array configuration results by design in Orientation 4 and $d_{\mathrm{RR}} = 2$cm.

C. Experimental Results on Natural Isolation

The power of the undesired self-interference term in (1) is

$$P_{\mathrm{I}} = \mathcal{E}\{\|\mathbf{H}_{\mathrm{RR}}\mathbf{x}_{\mathrm{R}}\|_2^2\} = \mathrm{tr}\{\mathbf{H}_{\mathrm{RR}}\mathbf{R}_{\mathbf{x}_{\mathrm{R}}}\mathbf{H}_{\mathrm{RR}}^H\}, \quad (3)$$

where $\mathbf{R}_{\mathbf{x}_{\mathrm{R}}} = \mathcal{E}\{\mathbf{x}_{\mathrm{R}}\mathbf{x}_{\mathrm{R}}^H\}$ denotes the covariance matrix of the relay transmit signal. Consequently, natural isolation (arising readily by deploying separated receive and transmit arrays) is given by $P_{\mathrm{tx}}/P_{\mathrm{I}} = 1/\|\mathbf{H}_{\mathrm{RR}}\|_F^2$ when assuming $\mathbf{R}_{\mathbf{x}_{\mathrm{R}}} = P_{\mathrm{tx}}\mathbf{I}$. In the following, we extend the SISO results of [23, Figs. 5,6] to the MIMO case (with slightly different definition for isolation).

Figure 3 shows the cumulative distribution function of natural isolation, $F_{P_{\mathrm{tx}}/P_{\mathrm{I}}}(\cdot)$, and the average natural isolation, $\mathcal{E}\{P_{\mathrm{tx}}/P_{\mathrm{I}}\}$, is illustrated in Fig. 4. With both configurations, the isolation varies more in the measured channels than in the case of Rayleigh channel model. We see that the isolation of NLOS channels varies more than that of LOS channels, but there is no significant difference in the average isolation. Transmit antenna orientation affects significantly both the variance and average value of the natural isolation.

For the separate array configuration, the average measured natural isolation closely follows a linear trend (in decibel scale) in terms of the antenna separation. With all orientations, the isolation is improved roughly 2–3dB per meter. By extrapolating the average natural isolation of Orientation 4 down to 2cm antenna separation, we observe 56dB isolation with the separate array configuration when it is made equivalent to the compact array configuration that achieves 36dB isolation. This additional 20dB isolation comes from the windowpanes.

In conclusion, we see that mere natural isolation may not be sufficient which motivates to develop and evaluate signal processing schemes that provide additional isolation.

978-1-4244-9848-2/11$26.00©2011 IEEE

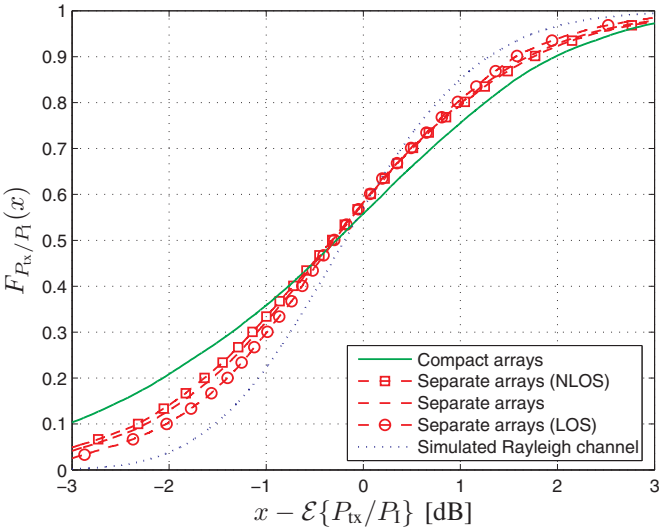

(a) Comparison of the array configurations.

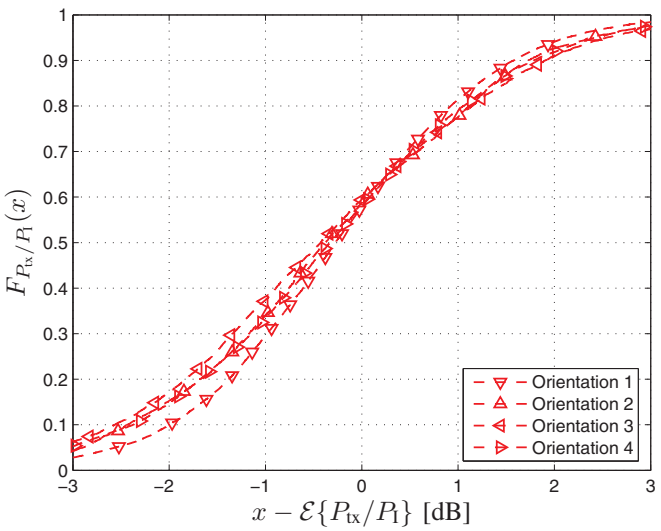

(b) Comparison of the orientations for the separate array configuration.

Fig. 3. The variation of natural isolation with different array configurations. For the compact array configuration $\mathcal{E}\{P_{\rm tx}/P_{\rm l}\} = 36.2$dB, and for the separate array configuration $\mathcal{E}\{P_{\rm tx}/P_{\rm l}\}$ depends on the distance $d_{\rm RR}$ between the relay antenna arrays as illustrated in Fig. 4.

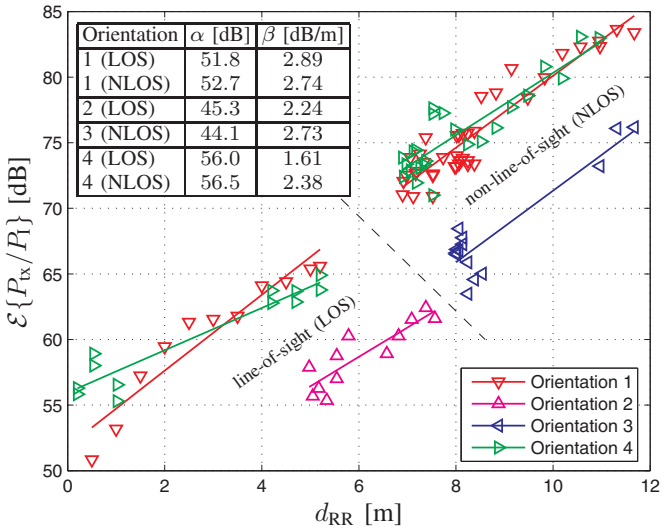

Fig. 4. Average natural isolation versus the distance $d_{\rm RR}$ from the transmit antenna array to the receive antenna array in the separate array configuration. The embedded table shows the parameters (intercept α and slope β) of the linear least-squares fit $\mathcal{E}\{P_{\rm tx}/P_{\rm l}\} \approx \alpha + \beta \cdot d_{\rm RR}$ [dB].

III. Optimal Eigenbeamforming for Self-Interference Suppression

We mitigate the relay self-interference in the spatial domain with the structure of Fig. 5. Ideally, suppression will turn the $N_{\rm rx} \times N_{\rm tx}$ relay into an interference-free $\hat{N}_{\rm rx} \times \hat{N}_{\rm tx}$ relay by using the combination of receive filter $\mathbf{G}_{\rm rx} \in \mathbb{C}^{\hat{N}_{\rm rx} \times N_{\rm rx}}$ and transmit filter $\mathbf{G}_{\rm tx} \in \mathbb{C}^{N_{\rm tx} \times \hat{N}_{\rm tx}}$ where $\hat{N}_{\rm rx} \leq N_{\rm rx}$, $\hat{N}_{\rm tx} \leq N_{\rm tx}$. Yet suppression should consume minimal number of the spatial dimensions which are scarce in general. Thus, we require also that the rows of $\mathbf{G}_{\rm rx}$ and the columns of $\mathbf{G}_{\rm tx}$ span orthonormal subspaces to guarantee that $\hat{N}_{\rm rx}$ input and $\hat{N}_{\rm tx}$ output streams are available for the MIMO relaying protocol.

With the spatial filters, the signal model of the relay is transformed from (1) to

$$\mathbf{x}_{\rm R} = \mathbf{G}_{\rm tx}\hat{\mathbf{x}}_{\rm R}, \tag{4}$$

$$\hat{\mathbf{y}}_{\rm R} = \mathbf{G}_{\rm rx}\mathbf{y}_{\rm R} = \underbrace{\mathbf{G}_{\rm rx}(\mathbf{H}_{\rm SR}\mathbf{x}_{\rm S} + \mathbf{n}_{\rm R})}_{\text{desired signal plus noise}} + \underbrace{\mathbf{G}_{\rm rx}\mathbf{H}_{\rm RR}\mathbf{G}_{\rm tx}\hat{\mathbf{x}}_{\rm R}}_{\text{interference signal}}. \tag{5}$$

After successful mitigation, any MIMO relaying protocol (with amplify-and-forward or decode-and-forward processing for example) can be used for generating $\hat{\mathbf{x}}_{\rm R} \in \mathbb{C}^{\hat{N}_{\rm tx} \times 1}$ based on $\hat{\mathbf{y}}_{\rm R} \in \mathbb{C}^{\hat{N}_{\rm rx} \times 1}$ while regarding the potential residual interference as an insignificant increment in the thermal noise level. Thereby, proper mitigation enables doubled symbol rate for the system when compared to the half-duplex alternative where the self-interference is avoided by allocating different time slots for relay reception and transmission.

Let us recall the standard singular value decomposition (SVD) and define it for the self-interference channel as

$$\mathbf{H}_{\rm RR} = \mathbf{U}_{\rm RR}\mathbf{\Sigma}_{\rm RR}\mathbf{V}_{\rm RR}^{H}, \tag{6}$$

where $\mathbf{U}_{\rm RR} \in \mathbb{C}^{N_{\rm rx} \times N_{\rm rx}}$ and $\mathbf{V}_{\rm RR} \in \mathbb{C}^{N_{\rm tx} \times N_{\rm tx}}$ are unitary matrices and $\mathbf{\Sigma}_{\rm RR} \in \mathbb{R}^{N_{\rm rx} \times N_{\rm tx}}$ is a diagonal matrix containing the singular values $\sigma_{\rm RR}[n] \geq 0$, $n = 1, \ldots, \min\{N_{\rm rx}, N_{\rm tx}\}$, of $\mathbf{H}_{\rm RR}$ in descending order. In the SVD, the rows of $\mathbf{U}_{\rm RR}^{H}$ (resp. the columns of $\mathbf{V}_{\rm RR}$) represent the set of orthonormal receive (resp. transmit) beamforming vectors. Thus, eigenbeamforming, i.e., eigenbeam selection, can be implemented with

$$\mathbf{G}_{\rm rx} = \mathbf{S}_{\rm rx}^{T}\mathbf{U}_{\rm RR}^{H} \quad \text{and} \quad \mathbf{G}_{\rm tx} = \mathbf{V}_{\rm RR}\mathbf{S}_{\rm tx}, \tag{7}$$

where $\mathbf{S}_{\rm rx}^{T} \in \{0,1\}^{\hat{N}_{\rm rx} \times N_{\rm rx}}$ and $\mathbf{S}_{\rm tx} \in \{0,1\}^{N_{\rm tx} \times \hat{N}_{\rm tx}}$ are generic row and column subset selection matrices, respectively. Finally, the combination of (6) and (7) yields a sparse interference channel matrix in (5):

$$\mathbf{G}_{\rm rx}\mathbf{H}_{\rm RR}\mathbf{G}_{\rm tx} = \mathbf{S}_{\rm rx}^{T}\mathbf{U}_{\rm RR}^{H}\mathbf{U}_{\rm RR}\mathbf{\Sigma}_{\rm RR}\mathbf{V}_{\rm RR}^{H}\mathbf{V}_{\rm RR}\mathbf{S}_{\rm tx} = \mathbf{S}_{\rm rx}^{T}\mathbf{\Sigma}_{\rm RR}\mathbf{S}_{\rm tx}$$

as $\mathbf{U}_{\rm RR}^{H}\mathbf{U}_{\rm RR} = \mathbf{I}$ and $\mathbf{V}_{\rm RR}^{H}\mathbf{V}_{\rm RR} = \mathbf{I}$ by definition.

978-1-4244-9848-2/11$26.00©2011 IEEE

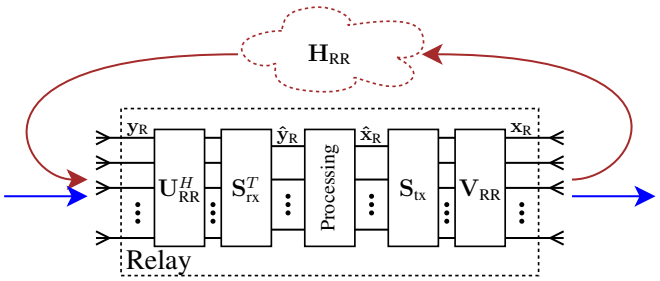

Fig. 5. Eigenbeamforming for self-interference suppression in full-duplex MIMO relays. The spatial receive and transmit filters are $\mathbf{G}_{\mathrm{rx}} = \mathbf{S}_{\mathrm{rx}}^T\mathbf{U}_{\mathrm{RR}}^H$ and $\mathbf{G}_{\mathrm{tx}} = \mathbf{V}_{\mathrm{RR}}\mathbf{S}_{\mathrm{tx}}$, respectively.

A. Optimization of Beam Selection Matrices

For optimal eigenbeamforming, we further need to optimize the choice of the beam selection matrices $\mathbf{S}_{\mathrm{rx}}$ and $\mathbf{S}_{\mathrm{tx}}$ such that the relay uses only the minimum eigenmodes of the self-interference channel. Accordingly, the power of the residual self-interference term in (5) can be minimized as

$$\begin{aligned} P_{\mathrm{I}} &= \min_{\mathbf{G}_{\mathrm{rx}},\mathbf{G}_{\mathrm{tx}}} \mathcal{E}\{\|\mathbf{G}_{\mathrm{rx}}\mathbf{H}_{\mathrm{RR}}\mathbf{G}_{\mathrm{tx}}\hat{\mathbf{x}}_{\mathrm{R}}\|_2^2\} \\ &= \min_{\mathbf{S}_{\mathrm{rx}},\mathbf{S}_{\mathrm{tx}}} P_{\mathrm{tx}}\|\mathbf{S}_{\mathrm{rx}}^T\mathbf{\Sigma}_{\mathrm{RR}}\mathbf{S}_{\mathrm{tx}}\|_F^2 \\ &= P_{\mathrm{tx}} \sum_{n=N_{\mathrm{rx}}+N_{\mathrm{tx}}-(\hat{N}_{\mathrm{rx}}+\hat{N}_{\mathrm{tx}})+1}^{\min\{N_{\mathrm{rx}},N_{\mathrm{tx}}\}} \sigma_{\mathrm{RR}}^2[n], \end{aligned} \tag{8}$$

when $\mathbf{R}_{\hat{\mathbf{x}}_{\mathrm{R}}} = \mathcal{E}\{\hat{\mathbf{x}}_{\mathrm{R}}\hat{\mathbf{x}}_{\mathrm{R}}^H\} = P_{\mathrm{tx}}\mathbf{I}$. Thus, optimal beam selection guarantees that the gain of the residual interference channel comprises $\hat{N}_{\mathrm{rx}} + \hat{N}_{\mathrm{tx}} - \max\{N_{\mathrm{rx}}, N_{\mathrm{tx}}\}$ (see Section III-C for the non-positive case) smallest singular values of $\mathbf{H}_{\mathrm{RR}}$.

The optimal beam selection matrices yielding (8) are not usually unique, but we may choose the solution that additionally minimizes $\mathcal{E}\{\|\mathbf{H}_{\mathrm{RR}}\mathbf{G}_{\mathrm{tx}}\hat{\mathbf{x}}_{\mathrm{R}}\|_2^2\} = P_{\mathrm{tx}}\|\mathbf{\Sigma}_{\mathrm{RR}}\mathbf{S}_{\mathrm{tx}}\|_F^2$ in order to reduce the risk of receiver front-end saturation. Thus, a recommended example solution can be formulated as

$$\mathbf{S}_{\mathrm{rx}}^T = \begin{bmatrix} \mathbf{I}_{N_{\mathrm{tx}}-\hat{N}_{\mathrm{tx}}} & \mathbf{0} & \mathbf{0} \\ \mathbf{0} & \mathbf{0} & \mathbf{I}_{\hat{N}_{\mathrm{rx}}+\hat{N}_{\mathrm{tx}}-N_{\mathrm{tx}}} \end{bmatrix} \text{ and } \mathbf{S}_{\mathrm{tx}} = \begin{bmatrix} \mathbf{0} \\ \mathbf{I}_{\hat{N}_{\mathrm{tx}}} \end{bmatrix}, \tag{9}$$

in which $\mathbf{I}_N$ denotes N-dimensional identity matrix and $\mathbf{0}$ represents different zero matrices with compatible dimensions. In addition, the rows of $\mathbf{S}_{\mathrm{rx}}^T$ and the columns of $\mathbf{S}_{\mathrm{tx}}$ may be permuted in any order to yield equivalent beam selection.

B. Comparison to the Scheme of [18]

Similar to our scheme, the suboptimal scheme proposed in [18] is based on the SVD of the self-interference channel. However, instead of minimizing the residual self-interference power, the proposed beam selection corresponds simply to

$$\mathbf{S}_{\mathrm{rx}}^T = \begin{bmatrix} \mathbf{0} & \mathbf{I}_{\hat{N}_{\mathrm{rx}}} \end{bmatrix} \text{ and } \mathbf{S}_{\mathrm{tx}} = \begin{bmatrix} \mathbf{0} \\ \mathbf{I}_{\hat{N}_{\mathrm{tx}}} \end{bmatrix}. \tag{10}$$

Note that only the symmetric case for which $N_{\mathrm{rx}} = N_{\mathrm{tx}}$ and $\hat{N}_{\mathrm{rx}} = \hat{N}_{\mathrm{tx}}$ is actually considered in [18], but we take the liberty of presenting comparison to the generalized version of the scheme with any N_{rx}, N_{tx}, $\hat{N}_{\mathrm{rx}}$ and $\hat{N}_{\mathrm{tx}}$.

With the suboptimal beam selection matrices of (10), the power of the residual self-interference term in (5) becomes

$$\begin{aligned} P_{\mathrm{I}} &= P_{\mathrm{tx}}\|\mathbf{S}_{\mathrm{rx}}^T\mathbf{\Sigma}_{\mathrm{RR}}\mathbf{S}_{\mathrm{tx}}\|_F^2 \\ &= P_{\mathrm{tx}} \sum_{n=\max\{N_{\mathrm{rx}}-\hat{N}_{\mathrm{rx}},N_{\mathrm{tx}}-\hat{N}_{\mathrm{tx}}\}+1}^{\min\{N_{\mathrm{rx}},N_{\mathrm{tx}}\}} \sigma_{\mathrm{RR}}^2[n], \end{aligned} \tag{11}$$

when $\mathbf{R}_{\hat{\mathbf{x}}_{\mathrm{R}}} = P_{\mathrm{tx}}\mathbf{I}$. The gain of the residual self-interference channel in (11) is higher than that in (8), because the sum consists of $\min\{N_{\mathrm{rx}} - \hat{N}_{\mathrm{rx}}, N_{\mathrm{tx}} - \hat{N}_{\mathrm{tx}}\}$ additional singular values of $\mathbf{H}_{\mathrm{RR}}$. In other words this means that, by optimizing the beam selection matrices, more spatial streams (higher $\hat{N}_{\mathrm{rx}}$ and/or $\hat{N}_{\mathrm{tx}}$) can be supported with the same P_{I}.

C. Special Case: Null-Space Projection

It is notable that optimal eigenbeamforming reduces to the null-space projection scheme studied in [12], [13] whenever

$$\hat{N}_{\mathrm{rx}} + \hat{N}_{\mathrm{tx}} \le \max\{N_{\mathrm{rx}}, N_{\mathrm{tx}}\} \le N_{\mathrm{rx}} + N_{\mathrm{tx}} - \mathrm{rk}\{\mathbf{H}_{\mathrm{RR}}\}. \tag{12}$$

Null-space projection directs relay reception and transmission to orthogonal subspaces, which is implemented with eigenbeamforming by choosing selection matrices that pick only off-diagonal elements of $\mathbf{\Sigma}_{\mathrm{RR}}$ (which are all zero) such that $\mathbf{S}_{\mathrm{rx}}^T\mathbf{\Sigma}_{\mathrm{RR}}\mathbf{S}_{\mathrm{tx}} = \mathbf{0}$. Thus, $\mathbf{G}_{\mathrm{rx}}\mathbf{H}_{\mathrm{RR}}\mathbf{G}_{\mathrm{tx}} = \mathbf{0}$ and $P_{\mathrm{I}} = 0$. The more loose condition in (12) corresponds to the case when the self-interference channel $\mathbf{H}_{\mathrm{RR}}$ is rank-deficient ($\sigma_{\mathrm{RR}}[n] = 0$ for some n). However, Fig. 6 shows the cumulative distribution function of condition number (in terms of the spectral norm),

$$\kappa\{\mathbf{H}_{\mathrm{RR}}\} = \|\mathbf{H}_{\mathrm{RR}}\|_2 \cdot \|\mathbf{H}_{\mathrm{RR}}^{-1}\|_2 = \frac{\sigma_{\mathrm{RR}}[1]}{\sigma_{\mathrm{RR}}[\min\{N_{\mathrm{rx}}, N_{\mathrm{tx}}\}]}, \tag{13}$$

for the measured channel data, which reveals that in practical installations $\mathrm{rk}\{\mathbf{H}_{\mathrm{RR}}\} = \min\{N_{\mathrm{rx}}, N_{\mathrm{tx}}\}$ (full rank) and the more strict condition in (12) should be applied.

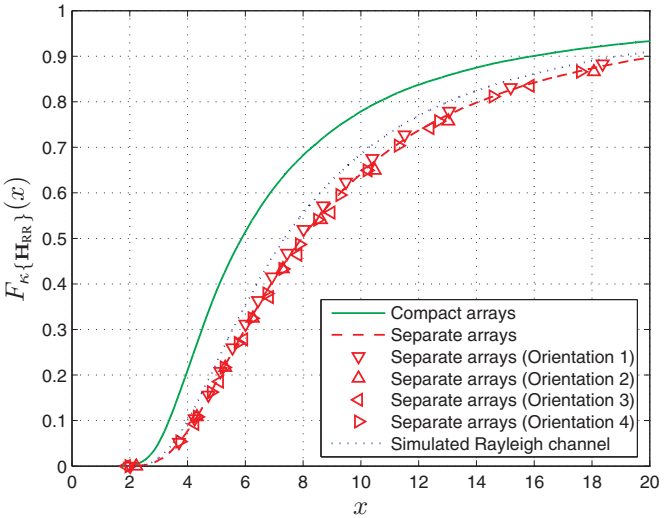

Fig. 6. The empirical distribution of the condition number. In particular, $\mathrm{rk}\{\mathbf{H}_{\mathrm{RR}}\} = 4$ (full rank) is observed for all measured and simulated channels. The average condition number, $\mathcal{E}\{\kappa\{\mathbf{H}_{\mathrm{RR}}\}\}$, is 9.2, 11.9, and 10.9 for compact arrays, separate arrays and simulated Rayleigh channels, respectively.

978-1-4244-9848-2/11$26.00©2011 IEEE

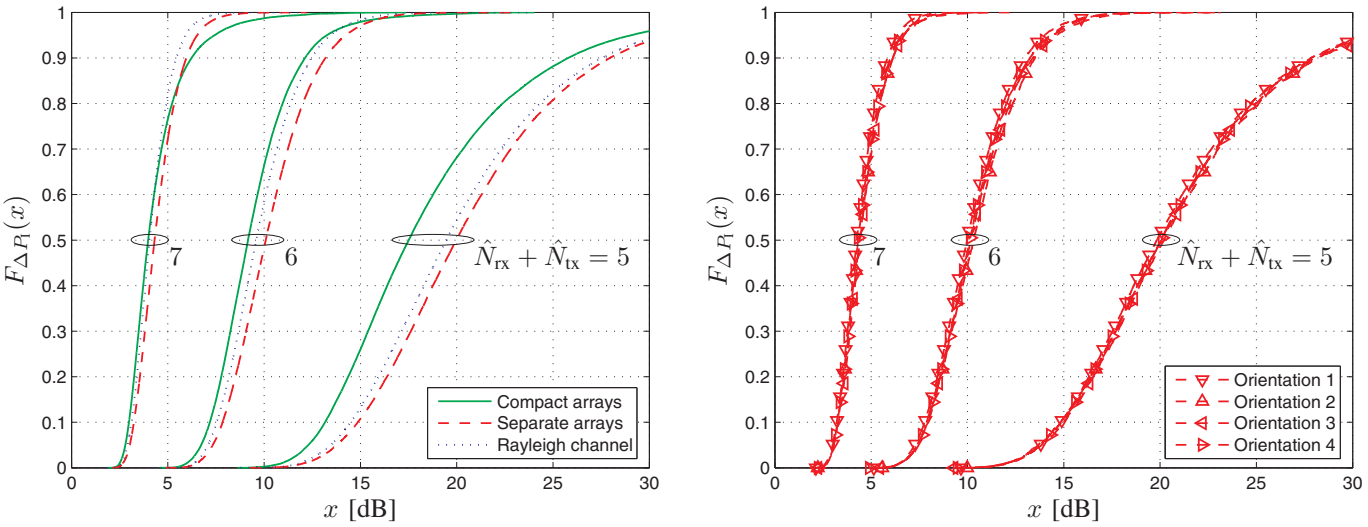

(a) Comparison of the array configurations.

(b) Comparison of the orientations for the separate array configuration.

Fig. 7. The variation of the additional isolation given by the proposed eigenbeamforming scheme with different number of input and output streams ($\hat{N}_\mathrm{rx}+\hat{N}_\mathrm{tx}$) when $N_\mathrm{rx}=N_\mathrm{tx}=4$. See Table I for the corresponding average values of isolation improvement.

IV. Experimental Results and Discussion

Based on the measurement data of [23], we evaluate next the isolation improvement, ΔP_I, which quantifies the additional isolation given by optimal eigenbeamforming w.r.t. the natural isolation of the practical channels:

$$\Delta P_\mathrm{I}=\frac{(P_\mathrm{tx}/P_\mathrm{I})\big|_\mathrm{suppression}}{(P_\mathrm{tx}/P_\mathrm{I})\big|_\mathrm{natural}}=\frac{\|\mathbf{H}_\mathrm{RR}\|_F^2}{\|\mathbf{S}_\mathrm{rx}^T\mathbf{\Sigma}_\mathrm{RR}\mathbf{S}_\mathrm{tx}\|_F^2}, \qquad (14)$$

for which $\mathbf{S}_\mathrm{rx}^T$ and $\mathbf{S}_\mathrm{tx}$ are given in (9). As explained in Section III-B, the scheme of [18] results in the same ΔP_I but with lower $\hat{N}_\mathrm{rx}$ and/or $\hat{N}_\mathrm{tx}$.

Channel variation over different relay locations and frequency makes ΔP_I a random variable. Thus, the analysis can be conducted in terms of the empirical cumulative distribution function $F_{\Delta P_\mathrm{I}}(\cdot)$ and the average improvement of isolation $\mathcal{E}\{\Delta P_\mathrm{I}\}$. Figure 7(a) illustrates how the channel variation affects the additional isolation given by the optimal eigenbeamforming scheme with the different array configurations. In general, the separate array configuration benefits more from eigenbeamforming than the compact array configuration. Figure 7(b) shows that the additional isolation is approximately the same with all orientations of the transmit antenna array. The difference of LOS and NLOS channels is even smaller (and thereby not shown). This is in contrast with the natural isolation for which the orientations behave rather differently.

As shown in Table I, 25–26dB, 10–11dB or 4–5dB additional isolation (depending on the array configuration) is achieved on average when supporting in total five, six or seven input and output streams ($\hat{N}_\mathrm{rx}+\hat{N}_\mathrm{tx}$), respectively. The channel data included few optimistic outliers (excluded from the average values) for which the additional isolation is extremely high (above 50dB). Note that if $\hat{N}_\mathrm{rx}+\hat{N}_\mathrm{tx}\leq 4$, optimal eigenbeamforming reduces to null-space projection and, thus, $\Delta P_\mathrm{I}\to\infty$, but in practice ΔP_I is still limited by imperfections in the side information needed for suppression [12], [13]. On the other hand, $\hat{N}_\mathrm{rx}+\hat{N}_\mathrm{tx}=8$ implies $\Delta P_\mathrm{I}=1$ which shows the fact that at least one spatial dimension needs to be reserved for suppression in order to reduce the self-interference at all.

Although the exact performance in simulated Rayleigh channels differs considerably from that in measured channels, the general observations are similar and the Rayleigh channel represents something that is in between the two different array configurations. Thus, the Rayleigh model could be reasonably used if measurement data is not available.

TABLE I
The average improvement of isolation $\mathcal{E}\{\Delta P_\mathrm{I}\}$ given by the proposed eigenbeamforming scheme with the different array configurations. The corresponding distributions are illustrated in Fig. 7(a).

$\hat{N}_\mathrm{rx}+\hat{N}_\mathrm{tx}$	Compact arrays	Separate arrays	Rayleigh channel
5	24.8dB	26.5dB	26.3dB
6	10.2dB	10.9dB	10.4dB
7	4.8dB	4.6dB	4.3dB

V. Conclusions

We studied a prospective concept to improve the performance of MIMO relay links: Full-duplex operation, which can render much higher spectral efficiency than conventional half-duplex operation, because it reserves the channel only once per each symbol forwarded by the relay. The main technical challenge, relay self-interference, can be initially tackled by using separated receive and transmit antenna arrays which provides natural isolation. If receiver front-end saturation is avoided, signal processing can improve isolation further. In this paper, we considered optimal eigenbeamforming and evaluated its performance using real-world measurement data.

978-1-4244-9848-2/11$26.00©2011 IEEE

REFERENCES

[1] B. Wang, J. Zhang, and A. Høst-Madsen, "On the capacity of MIMO relay channels," *IEEE Transactions on Information Theory*, vol. 51, no. 1, pp. 29–43, January 2005.

[2] A. Høst-Madsen and J. Zhang, "Capacity bounds and power allocation for wireless relay channels," *IEEE Transactions on Information Theory*, vol. 51, no. 6, pp. 2020–2040, June 2005.

[3] G. Kramer, M. Gastpar, and P. Gupta, "Cooperative strategies and capacity theorems for relay networks," *IEEE Transactions on Information Theory*, vol. 51, no. 9, pp. 3037–3063, September 2005.

[4] M. Yuksel and E. Erkip, "Multiple-antenna cooperative wireless systems: A diversity–multiplexing tradeoff perspective," *IEEE Transactions on Information Theory*, vol. 53, no. 10, pp. 3371–3393, October 2007.

[5] Y. Liang, V. V. Veeravalli, and H. V. Poor, "Resource allocation for wireless fading relay channels: Max-min solution," *IEEE Transactions on Information Theory*, vol. 53, no. 10, pp. 3432–3453, October 2007.

[6] T. Riihonen, S. Werner, and R. Wichman, "Comparison of full-duplex and half-duplex modes with a fixed amplify-and-forward relay," in *Proc. IEEE Wireless Communications and Networking Conference*, April 2009.

[7] T. Riihonen, S. Werner, R. Wichman, and E. Zacarias B., "On the feasibility of full-duplex relaying in the presence of loop interference," in *Proc. 10th IEEE Workshop on Signal Processing Advances in Wireless Communications*, June 2009.

[8] T. Riihonen, S. Werner, and R. Wichman, "Rate–interference trade-off between duplex modes in decode-and-forward relaying," in *Proc. 21st IEEE International Symposium on Personal, Indoor and Mobile Radio Communications*, September 2010.

[9] J. Sangiamwong, T. Asai, J. Hagiwara, Y. Okumura, and T. Ohya, "Joint multi-filter design for full-duplex MU-MIMO relaying," in *Proc. IEEE 69th Vehicular Technology Conference*, April 2009.

[10] Y. Y. Kang and J. H. Cho, "Capacity of MIMO wireless channel with full-duplex amplify-and-forward relay," in *Proc. IEEE 20th International Symposium on Personal, Indoor and Mobile Radio Communications*, September 2009.

[11] J. Ma, G. Y. Li, J. Zhang, T. Kuze, and H. Iura, "A new coupling channel estimator for cross-talk cancellation at wireless relay stations," in *Proc. IEEE Global Communications Conference*, December 2009.

[12] T. Riihonen, S. Werner, and R. Wichman, "Spatial loop interference suppression in full-duplex MIMO relays," in *Proc. 43rd Annual Asilomar Conference on Signals, Systems, and Computers*, November 2009.

[13] ——, "Residual self-interference in full-duplex MIMO relays after null-space projection and cancellation," in *Proc. 44th Annual Asilomar Conference on Signals, Systems, and Computers*, November 2010.

[14] D. W. Bliss, P. A. Parker, and A. R. Margetts, "Simultaneous transmission and reception for improved wireless network performance," in *Proc. IEEE 14th Workshop on Statistical Signal Processing*, August 2007.

[15] B. Chun, E.-R. Jeong, J. Joung, Y. Oh, and Y. H. Lee, "Pre-nulling for self-interference suppression in full-duplex relays," in *Proc. APSIPA Annual Summit and Conference*, October 2009.

[16] B. Chun and Y. H. Lee, "A spatial self-interference nullification method for full duplex amplify-and-forward MIMO relays," in *Proc. IEEE Wireless Communications and Networking Conference*, April 2010.

[17] A. Hazmi, J. Rinne, and M. Renfors, "Diversity based DVB-T in-door repeater in slowly mobile loop interference environment," in *Proc. 10th International OFDM-Workshop*, August–September 2005.

[18] P. Larsson and M. Prytz, "MIMO on-frequency repeater with self-interference cancellation and mitigation," in *Proc. IEEE 69th Vehicular Technology Conference*, April 2009.

[19] S. Sohaib and D. K. C. So, "Asynchronous polarized cooperative MIMO communication," in *Proc. IEEE 69th Vehicular Technology Conference*, April 2009.

[20] T. Riihonen, S. Werner, and R. Wichman, "Optimized gain control for single-frequency relaying with loop interference," *IEEE Transactions on Wireless Communications*, vol. 8, no. 6, pp. 2801–2806, June 2009.

[21] T. Riihonen, K. Haneda, S. Werner, and R. Wichman, "SINR analysis of full-duplex OFDM repeaters," in *Proc. IEEE 20th International Symposium on Personal, Indoor and Mobile Radio Communications*, September 2009.

[22] P. Persson, M. Coldrey, A. Wolfgang, and P. Bohlin, "Design and evaluation of a 2 x 2 MIMO repeater," in *Proc. 3rd European Conference on Antennas and Propagation*, March 2009.

[23] K. Haneda, E. Kahra, S. Wyne, C. Icheln, and P. Vainikainen, "Measurement of loop-back interference channels for outdoor-to-indoor full-duplex radio relays," in *Proc. 4th European Conference on Antennas and Propagation*, April 2010.

978-1-4244-9848-2/11$26.00©2011 IEEE